

Optimizing Promoters and Subcellular Localization for Constitutive Transgene Expression in *Marchantia polymorpha*

Sze Wai Tse^{1,†}, Davide Annese^{1,†}, Facundo Romani¹, Fernando Guzman-Chavez^{1,2}, Ignacy Bonter¹, Edith Forestier¹, Eftychios Frangedakis¹ and Jim Haseloff^{1,*}

¹Department of Plant Sciences, University of Cambridge, Cambridge CB2 3EA, UK

²CONAHcyT, Instituto de Investigaciones Biomédicas, Universidad Nacional Autónoma de México (UNAM), CDMX 04510, México

[†]The first two authors contributed equally to this work.

*Corresponding author: E-mail, jh295@cam.ac.uk

(Received 4 April 2024; Accepted 31 May 2024)

Marchantia polymorpha has become an important model system for comparative studies and synthetic biology. The systematic characterization of genetic elements would make heterologous gene expression more predictable in this test bed for gene circuit assembly and bioproduction. Yet, the toolbox of genetic parts for *Marchantia* includes only a few constitutive promoters that need benchmarking to assess their utility. We compared the expression patterns of previously characterized and new constitutive promoters. We found that driving expression with the double enhancer version of the cauliflower mosaic virus 35S promoter ($_{pro}35S \times 2$) provided the highest yield of proteins, although it also inhibits the growth of transformants. In contrast, promoters derived from the *Marchantia* genes for ETHYLENE RESPONSE FACTOR 1 and the CLASS II HOMEODOMAIN-LEUCINE ZIPPER protein drove expression to higher levels across all tissues without a growth penalty and can provide intermediate levels of gene expression. In addition, we showed that the cytosol is the best subcellular compartment to target heterologous proteins for higher levels of expression without a significant growth burden. To demonstrate the potential of these promoters in *Marchantia*, we expressed *RUBY*, a polycistronic betalain synthesis cassette linked by P2A sequences, to demonstrate coordinated expression of metabolic enzymes. A heat-shock-inducible promoter was used to further mitigate growth burdens associated with high amounts of betalain accumulation. We have expanded the existing tool kit for gene expression in *Marchantia* and provided new resources for the *Marchantia* research community.

Keywords: Betalain • *Marchantia polymorpha* • Metabolic engineering • Promoter • Recombinant protein • Synthetic biology

Introduction

Promoters play a key role in controlling the levels and cell specificity of gene expression. In plants, native, heterologous and synthetic promoters (Villao-Uzho et al. 2023), have been characterized for their ability to drive higher levels of expression, primarily in transient expression systems such as *Nicotiana benthamiana* (Engler et al. 2014, Brückner et al. 2015, Cai et al. 2020, Tian et al. 2022). However, studies rarely describe native promoters for stable transformation, and the majority focus on the model species *Arabidopsis thaliana* (Holtorf et al. 1995, Han et al. 2015, Jiang et al. 2018, Yang and Nemhauser 2023). As expression levels associated with promoters are not easily transferable between plant species, the lack of promoter characterization in non-model systems has become a limitation for the design and assembly of genetic circuits.

Marchantia polymorpha, an emerging land plant model (Bowman et al. 2022), is ideally suited to address this shortcoming, thanks to its short cycle of growth and reproduction, remarkable regenerative capacity and the extensive set of available experimental tools (Ishizaki et al. 2015, Sauret-Güeto et al. 2020). *Marchantia* also produces clonal offspring called gemmae, making it suitable for large-scale comparative studies due to the ease of imaging at a cellular level and rapid growth. Additionally, nuclear transformation can be performed on a large scale, enabling the generation of hundreds of lines within 3–4 weeks, in contrast to systems like *A. thaliana* or *N. benthamiana*, which may take months (Ishizaki et al. 2008, 2015, Sauret-Güeto et al. 2020, Romani et al. 2024). The *Marchantia* system has potential as a platform for facile testing of promoters for genetic and biotechnological applications.

A number of studies have explored *Marchantia* as a platform for the production of recombinant proteins (Frangedakis et al. 2021) and metabolites (Takemura et al. 2013), but

comparative studies of constitutive promoters in *Marchantia* are scarce (Althoff et al. 2014). Such work is necessary because some heterologous promoters in *Marchantia* do not perform as expected. For instance, the widely used cauliflower mosaic virus 35S promoter ($_{pro}35S$) showed a non-homogenous expression pattern in *Marchantia* (Amack and Antunes 2020), as previously seen in other bryophyte species such as *Physcomitrium patens* (Finka et al. 2008, Saidi et al. 2009), while the *Agrobacterium tumefaciens* Nopaline Synthase promoter ($_{pro}NOS$) is poorly functional in *Marchantia* (Ishizaki et al. 2015). In addition, *Marchantia* promoters do not necessarily perform well in transformed *N. benthamiana* leaves and BY2 suspension cell cultures (Tian et al. 2022), confirming that promoter activity cannot be reliably extrapolated between divergent plants such as angiosperms and liverworts.

Four promoters with broad patterns of expression are commonly used in *Marchantia*. The native *ELONGATION FACTOR 1 α* promoter ($_{pro}MpEF1\alpha$) (Althoff et al. 2014), the single and double enhancer versions of the cauliflower mosaic virus 35S promoter [$_{pro}35S$ (Althoff et al. 2014) and $_{pro}35S \times 2$ (Ishizaki et al. 2015)] and the *Marchantia* UBIQUITIN-CONJUGATING ENZYME E2 promoter ($_{pro}MpUBE2$) (Sauret-Güeto et al. 2020). It was shown before that $_{pro}MpEF1\alpha$ can drive the expression of high levels of recombinant protein but its expression pattern is stronger near the apical notch, while the single and double enhancer versions of the cauliflower mosaic virus 35S promoter show comparatively weaker expression near the apical notch (Althoff et al. 2014, Ishizaki et al. 2015). As an alternative, $_{pro}MpUBE2$ showed a more even expression pattern across the gemma (Sauret-Güeto et al. 2020). A set of five promoters was released as part of the OpenPlant tool kit (Sauret-Güeto et al. 2020) as synthetic parts compatible with modular cloning (Patron et al. 2015) but systematic comparison is lacking. Recently, a large set of promoters derived from transcription factors in *Marchantia* has been published (Romani et al. 2024), providing a new pool of candidates for selection of promoters that drive strong and ubiquitous expression.

Besides promoter selection, maximizing expression can be achieved by targeting the protein to specific compartments such as the apoplast, chloroplast and endoplasmic reticulum (ER) (Feng et al. 2022, Liu and Timko 2022), but this strategy remains largely unexplored in *Marchantia*. During transient expression in *N. benthamiana*, targeting to the apoplast was reported to produce human growth hormone at levels up to 10% of total soluble protein (Gils et al. 2005), and anti-hen egg white lysozyme nanobody up to 30% of the total leaf protein (Teh and Kavanagh 2010). Furthermore, post-translational targeting to the chloroplast yielded 0.1–11% of recombinant proteins in various systems (Muthamilselvan et al. 2019). As for targeting to the ER, the formation of protein bodies induced by high levels of accumulation of recombinant proteins can further boost the yield up to 40–50% of total soluble content (Bankar et al. 2009, Saberianfar et al. 2015). Transgene expression from the *Marchantia* chloroplast genome produced up to 400–500 $\mu\text{g/g}$ (15% of total soluble protein) FW of mTurquoise2

fluorescent protein (Frangedakis et al. 2021), but yields of protein expressed from the nuclear genome, which allows for diverse subcellular targeting, remain poorly characterized.

We characterized the relative strengths of a collection of nine putative constitutive promoters, four from the OpenPlant tool kit and five native promoters derived from the transcription factors. We compared levels of accumulation for proteins with different subcellular targeting, the first such data for *Marchantia*. Furthermore, we also tested the expression of the betalain biosynthesis cassette RUBY (He et al. 2020) and quantified the yield of betanin. This provided quantitative characterization of promoters that will be useful for gene circuit assembly, and a demonstration of the *Marchantia* system as a test bed for metabolic engineering and yield benchmarks.

Results

Expression patterns of constitutive promoters

We aimed to develop novel constitutive promoter elements for *Marchantia*, which would allow high levels of transgene expression as well as exhibit homogenous expression throughout the thallus. We examined a collection of ~ 400 putative transcription factor promoter regions fused to the mVenus-N7 reporter (Fig. 1A) (Romani et al. 2024). We screened for promoters that exhibited bright mVenus fluorescence across all tissue types in day 0 gemmae and day 7 plants. This allowed us to pick five candidates: *Marchantia* ETHYLENE RESPONSE FACTOR 1 ($_{pro}MpERF1$), $_{pro}MpERF4$, $_{pro}MpC2HDZ$, $_{pro}Mp1R-MYB7$ and $_{pro}MpR2R3-MYB9$.

We first compared the expression patterns of the five candidates with $_{pro}35S$ and $_{pro}35S \times 2$, $_{pro}MpEF1\alpha$ and $_{pro}MpUBE2$ reporter fusions in day 0 gemmae and day 7 plants. These candidates were selected as they all appeared to drive expression of mVenus-N7 across all tissue types and strongly during a preliminary screening of day 0 gemmae. Consistent with previously reported data (Althoff et al. 2014), for all time points, $_{pro}35S$ and $_{pro}35S \times 2$ plants showed low expression in the cells close to the apical notch (Fig. 1B), in contrast to $_{pro}MpEF1\alpha$, where the strongest expression was observed in cells close to the apical notch. Expression of the $_{pro}MpUBE2$ -driven reporter was ubiquitous across all tissue types from gemmae at day 0 to day 7 plants, as it was for $_{pro}MpERF1$ and $_{pro}MpR2R3-MYB9$ (Fig. 1B). The expression patterns of $_{pro}Mp1R-MYB7$, $_{pro}MpC2HDZ$ and $_{pro}MpERF4$ reporters were also ubiquitous across all tissue types (Supplementary Fig. S1).

Benchmarking promoters for heterologous expression

In order to compare expression levels for the candidate constitutive promoters, we quantified nuclear-localized mVenus-N7 reporter protein levels in 3-week-old plants. The constitutive $_{pro}35S \times 2$ reported the highest protein yield: up to 52 $\mu\text{g/g}$ FW, although the level of expression between different independent

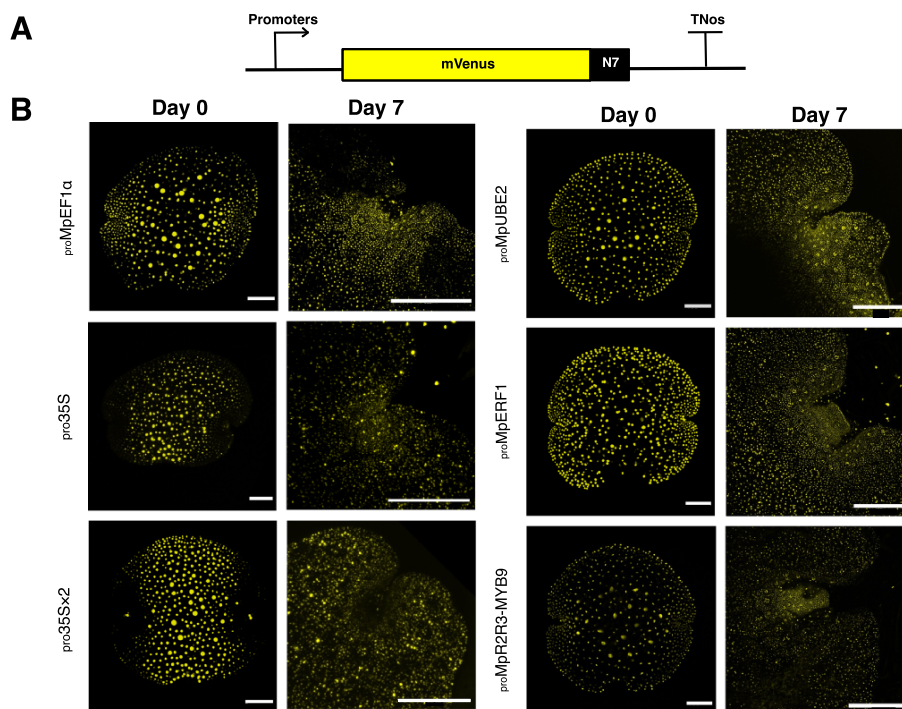


Fig. 1 Expression pattern of mVenus-N7 reporter driven by different promoters in day 0 *Marchantia* gemmae and day 7 plants from different promoter:mVenus-N7 lines. (A) Schematic representation of the promoter:mVenus-N7 constructs. (B) Confocal microscopy Images, mVenus-N7 signal shown light coloured. Scale bar for day 0 plants = 100 μm . Scale bar for day 7 plants = 400 μm . Gene IDs: MpERF1 (Mp1g20040), R2R3-MYB TRANSCRIPTION FACTOR 9 (R2R3-MYB9, Mp5g14610), ELONGATION FACTOR 1 α (MpEF1 α , Mp3g23400) and MpUBE2 (Mp5g21800).

transformants varied, likely due to T-DNA insert number, positional effect or post-transcriptional silencing. Among the newly characterized ubiquitous promoters, $\text{pro}_{\text{MpERF1}}$ and $\text{pro}_{\text{MpC2HDZ}}$ produced an average of 5–10 $\mu\text{g/g}$ FW of mVenus-N7 in reporter lines, which is similar to $\text{pro}_{35\text{S} \times 2}$, $\text{pro}_{35\text{S}}$ and $\text{pro}_{\text{MpEF1}\alpha}$ reporter lines (**Fig. 2B**). Whereas $\text{pro}_{\text{MpR2R3-MYB9}}$ and $\text{pro}_{\text{MpR2R3-MYB9}}$ can provide lower levels of transgene expression, $\text{pro}_{\text{MpUBE2}}$ has an intermediate performance.

To understand the relationship between protein yield and the potential growth burden on plants, we measured the size of 2-week-old plants. Variation between individual biological replicates and lines of the same construct can be seen (**Fig. 2C**). Lines with higher protein expression levels, such as $\text{pro}_{35\text{S} \times 2}$ and $\text{pro}_{\text{MpEF1}\alpha}$ lines, had significantly smaller sizes (~60% smaller than plants from other lines) at the same age compared to other plants (**Fig. 2D**), which suggested that high levels of recombinant protein accumulation are associated with growth defects.

Subcellular localization and growth burden

To explore if subcellular localization of the protein product could differentially impact yield as well as growth of the transgenic plant, we tested a series of peptide fusions to drive protein accumulation to different subcellular compartments in *Marchantia*: apoplast, plastids, plasma membrane, nucleus and cytosol (**Fig. 3A**). The reporter mTurquoise2

was preferred over mVenus as it allowed comparison with the same reporter expressed from the chloroplast genome (Frangedakis et al. 2021). We used the plasma membrane localization signal from the Arabidopsis gene AT3G05890 (LTI6b), the nuclear localization signal from the Arabidopsis ankyrin-like protein, AT4G19150 (N7) and the chloroplast signal peptide from *Marchantia* SIG2 Mp4g13380 (Sauret-Güeto et al. 2020). We also adapted the N-terminal transit peptide (PEC) of an apple pectinase (GenBank accession: L27743.1) (Marrillonnet et al. 2004) for apoplast targeting in *Marchantia*. Imaging of day 0 gemmae confirmed that the mTurquoise2 protein in all lines appeared to be located in the expected compartment (**Fig. 3B**). For $\text{pro}_{\text{MpEF1}\alpha}:\text{PEC-mTurquoise2}$ lines, we confirmed the targeting to the apoplast by plasmolysis, with the $\text{pro}_{\text{MpEF1}\alpha}:\text{mTurquoise2}$ line as a negative control (Supplementary Fig. S2). Treatment with a high level of osmoticum caused the plasma membrane and cell contents to draw away from the cell walls, seen in plasmolyzed cells containing $\text{pro}_{\text{MpEF1}\alpha}:\text{mTurquoise2}$, whereas plasmolyzed cells from $\text{pro}_{\text{MpEF1}\alpha}:\text{PEC-Turquoise2}$ expressing gemmae showed residual fluorescence associated with the cell wall regions in the apoplast. The bulk of the fluorescent protein observed in untreated $\text{pro}_{\text{MpEF1}\alpha}:\text{PEC-Turquoise2}$ gemmae was associated with the outer part of the cell, possibly including the plasma membrane, and a portion of the PEC-mTurquoise2 protein was localized to the apoplast as intended.

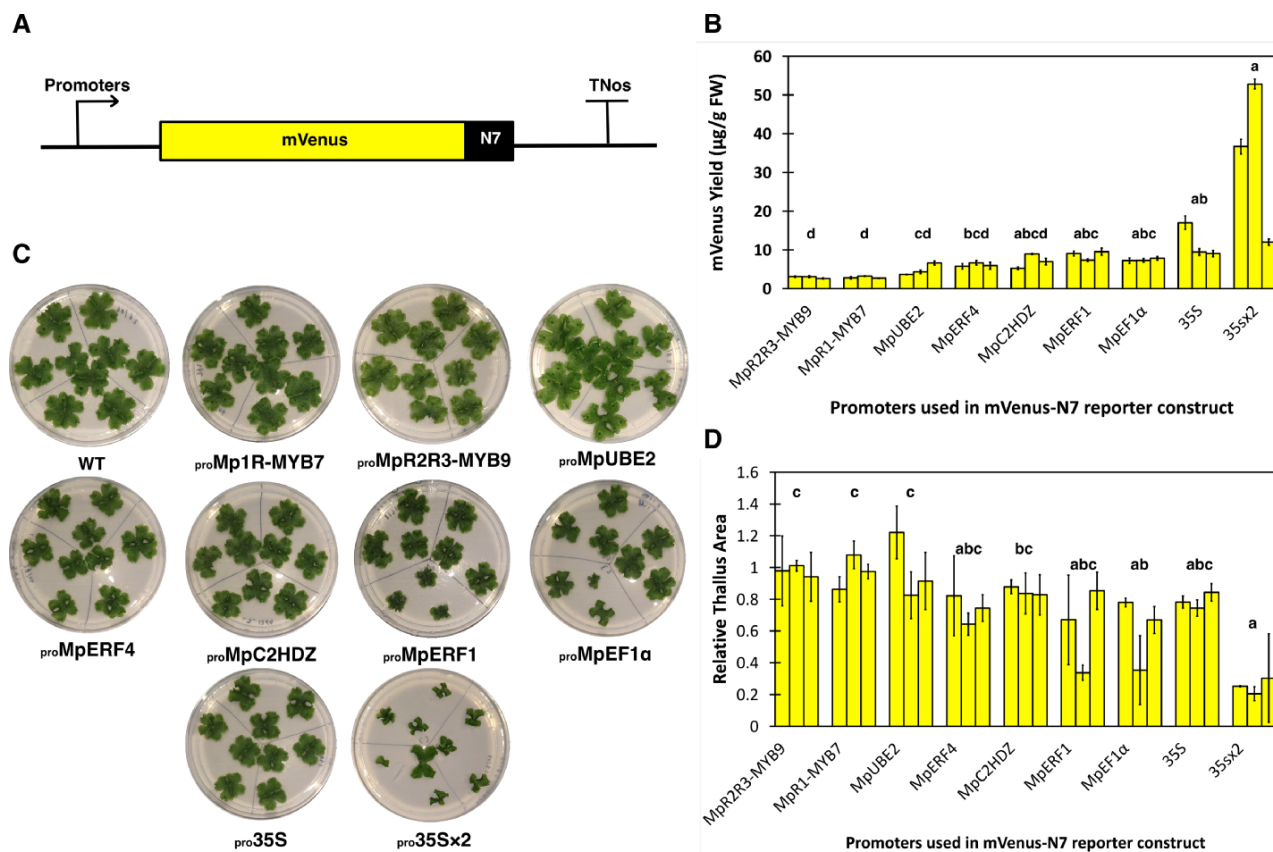


Fig. 2 Expression level of mVenus-N7 in different promoter lines and relative size estimation of plants from different promoter:mVenus-N7 lines. (A) Schematic representation of the promoter:mVenus-N7 constructs. (B) mVenus-N7 expressed in different promoter lines in 3-week-old plants, in $\mu\text{g/g}$ FW. (C) Images of 2-week-old WT and different promoter line plants grown in 9-cm Petri dishes 0.5 \times Gamborg B-5 basal medium supplemented with 0.5% (w/v) sucrose. The plates were divided into three portions, and on each portion grew three gemmae derived from the same independent transformant of that promoter construct. (D) Relative thallus size (the ratio of sizes of promoter line plants: average size of WT plants) of different promoter line plants (2-week-old). In B and D, each bar represents an independent transformant for that promoter construct, and error bars represent standard deviation between three biological replicates. Letters above the bars indicate statistically significant differences between the different promoter:mVenus-N7 lines (Dunn's test; $P < 0.05$).

We then extracted and quantified the protein yields in all lines with mTurquoise2 targeted to different cellular compartments. $\text{proMpef1}\alpha\text{:mTurquoise2}$ lines, where mTurquoise2 is targeted to the cytosol, accumulated on average the highest amount of mTurquoise2 ($\sim 30 \mu\text{g/g}$ FW). The average yield from $\text{proMpef1}\alpha\text{:mTurquoise2-LTI6b}$ lines was the second highest at $\sim 25 \mu\text{g/g}$ FW, significantly higher than those for $\text{proMpef1}\alpha\text{:mTurquoise2-N7}$, $\text{proMpef1}\alpha\text{:SIG2-mTurquoise2}$ and $\text{proMpef1}\alpha\text{:PEC-mTurquoise2-LTI6b}$ (all $\sim 10 \mu\text{g/g}$ FW). Estimation of the sizes of 2-week-old plants showed that $\text{proMpef1}\alpha\text{:mTurquoise2-LTI6b}$ plants were significantly smaller ($\sim 70\%$) than all other plants apart from $\text{proMpef1}\alpha\text{:SIG2-mTurquoise2}$ plants (Fig. 4C, D). This suggests that in *Marchantia*, the cytosol appears to be the best-performing compartment for mTurquoise2 production, while targeting recombinant protein to the plasma membrane accrued more growth penalties than retaining the protein in the cytosol.

To test the combined effects of a strong promoter and cytosolic targeting of the reporter protein on the growth of transgenic plants, we employed the promoter that allowed the highest accumulation of mVenus-N7 ($\text{pro35S} \times 2$) with the sub-cellular localization that gives the highest mTurquoise2 yield (cytosol) to generate a $\text{pro35S} \times 2\text{:mTurquoise2}$ line and compare its performance with a $\text{proMpef1}\alpha\text{:mTurquoise2}$ line. We confirmed that the $\text{pro35S} \times 2\text{:mTurquoise2}$ plants have a significantly higher ($\sim 40\%$) mTurquoise2 yield, yet their sizes were similar to $\text{proMpef1}\alpha\text{:mTurquoise2}$ plants. Cytosolic targeting allows high reporter protein yields while minimizing negative impacts on plant growth (Supplementary Fig. S3).

Engineering betalain biosynthesis in *Marchantia*

Fluorescent proteins are very useful to visualize and measure protein accumulation in prototype systems, but are not a direct model for expression and performance of multienzyme

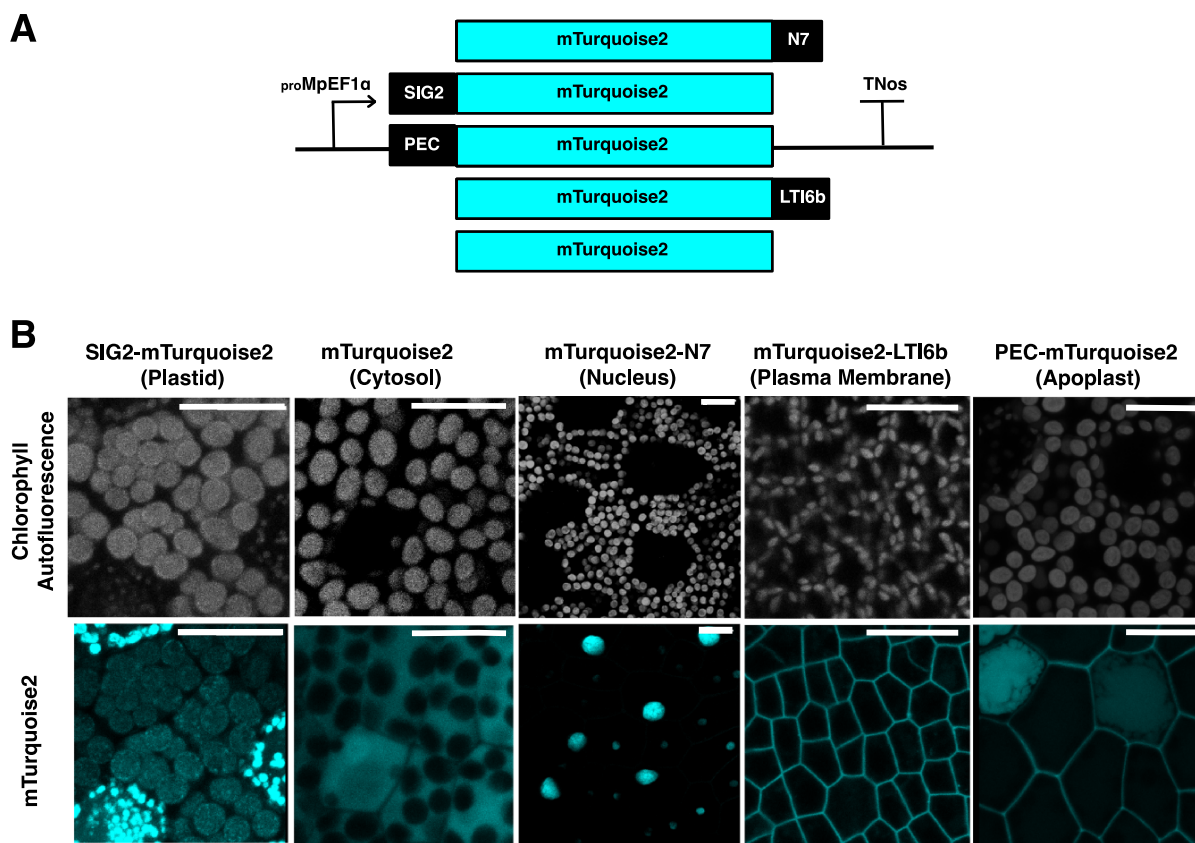


Fig. 3 Expression pattern of mTurquoise2 reporter driven by $proMpEF1\alpha$ in day 0 *Marchantia* gemmae targeted to different subcellular locations. (A) Schematic representation of different subcellular targeting $proMpEF1\alpha:mTurquoise2$ constructs. N7: nuclear localization signal from the Arabidopsis ankyrin-like protein, AT4G19150. LTI6b: plasma membrane localization signal from the Arabidopsis gene AT3G05890. SIG2: chloroplast signal peptide from *Marchantia* SIG2 Mp4g13380.1. PEC: the N-terminal transit peptide (PEC) of an apple pectinase (GenBank accession: L27743.1). (B) Confocal microscopy images, where mTurquoise2 signal is shown light coloured and chlorophyll autofluorescence shown in gray. Scale bar = 20 μm . For labels of each construct, construct names labeled on top; intended subcellular localization is marked in bracket at the bottom.

pathways and product accumulation. As an additional test, we used six promoters: $pro35S$, $proMpR2R3-MYB9$, $proMpERF1$, $proMpUBE2$, $pro35S \times 2$ and $proMpEF1\alpha$ to express the *RUBY* cassette. Betalains are a group of plant pigments synthesized from the amino acid tyrosine. They include betanin, which can be used as a bright red food colorant (Grützner et al. 2021). The *RUBY* cassette contains the coding sequences for P450 oxygenase CYP76AD1 (CYP76/AD1), L-DOPA 4,5-dioxygenase (DODA) and glucosyltransferase (GT), three enzymes required for betanin synthesis from beetroot (*Beta vulgaris*) separated by the P2A peptide (He et al. 2020) (Fig. 5A), a viral sequence that allows expression of multiple genes in polycistronic vectors by ribosome ‘skipping’ (de Felipe et al. 2010). For these enzymes, CYP76/AD1 is localized to the ER in yeast (DeLoache et al. 2015), and DODA and GT are localized to the cytoplasm/nucleus in plants (Chen et al. 2017). This cassette has been expressed successfully in many species (Zhao 2023).

We first demonstrated that the *RUBY* cassette is functional in *Marchantia* and produced betanin. Light microscopy of day 0 gemmae from the $pro35S:RUBY$ line confirmed betanin

accumulation, indicated by the presence of the signature bright red color (Fig. 5B). The absorption peak at 538-nm for extracts from the $pro35S:RUBY$ line confirmed that the pigment produced was betanin (Fig. 5D).

In addition to $pro35S$, we expressed the *RUBY* cassette in *Marchantia* with five other constitutive promoters: $proMpR2R3-MYB9$, $proMpERF1$, $proMpUBE2$, $pro35S \times 2$ and $proMpEF1\alpha$. The yields show the same pattern observed with the mVenus reporter lines. A maximum amount of $\sim 640 \mu\text{g/g}$ FW of betanin was obtained in 3-week-old $pro35S \times 2:RUBY$ plants, significantly higher than all other lines except $pro35S:RUBY$ (Fig. 6B). The yields of betanin were negatively correlated with the size of 2-week-old plants (Fig. 6D), similar to the effects of overexpression seen in mVenus-N7 lines.

To reduce the adverse effect of betanin production on plant growth, we drove expression of *RUBY* under the *Marchantia* native heat-shock promoter $proMpHSP17.8A1$ (Nishihama et al. 2016). This allows the production of betanin once the plants have accumulated enough biomass (Dugdale et al. 2013). To do so, the plants were placed in a 37°C incubator for 2 and

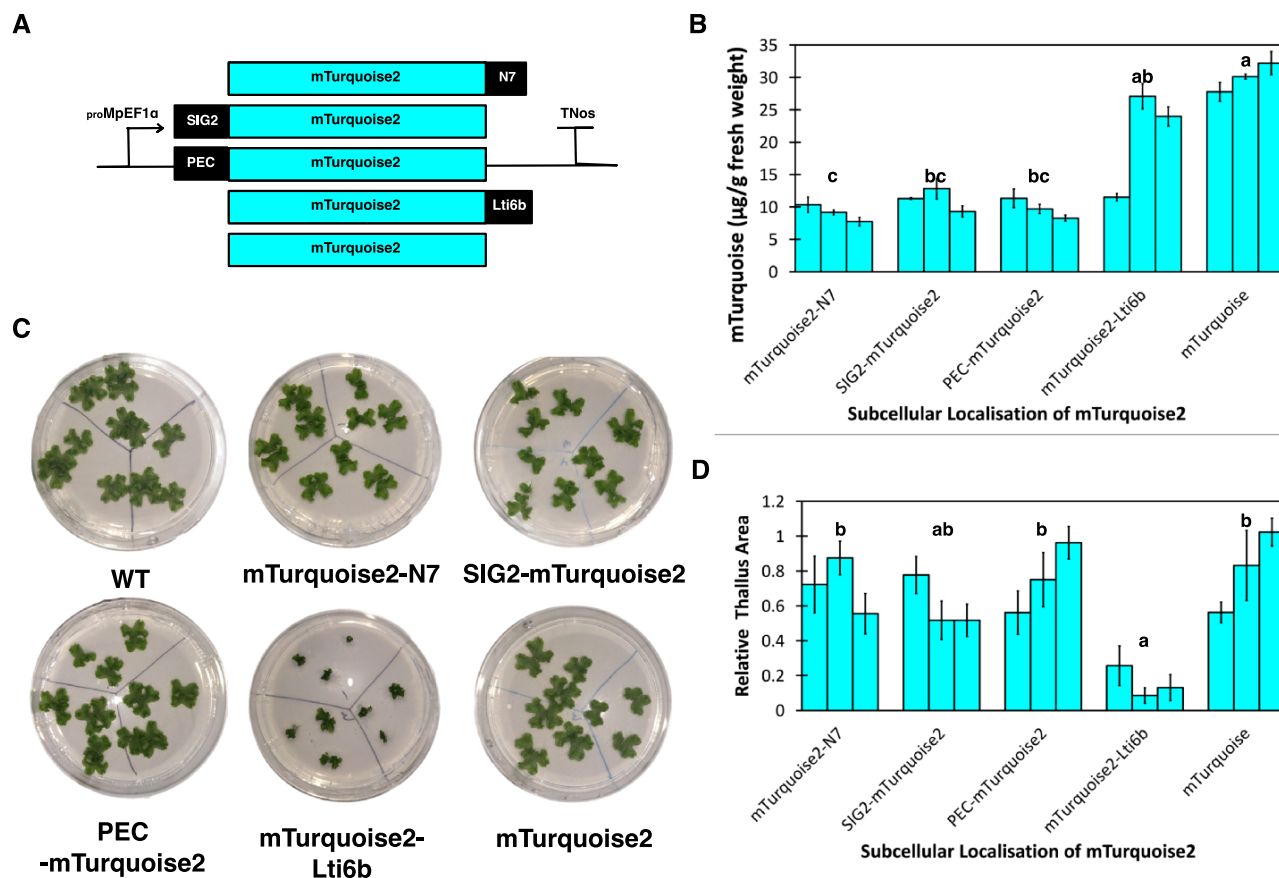


Fig. 4 Expression level of mTurquoise2 in different subcellular-targeting lines and relative size estimation of plants from different subcellular targeting $\text{proMpEF1}\alpha\text{:mTurquoise2}$ lines. (A) Schematic representation of different subcellular targeting $\text{proMpEF1}\alpha\text{:mTurquoise2}$ constructs. (B) mTurquoise2 expressed in different subcellular-targeting lines in 3-week-old plants, in $\mu\text{g/g}$ FW. (C) Images of 2-week-old WT and different subcellular-targeting line plants grown in 9-cm Petri dishes in 0.5x Gamborg B-5 basal medium. The plates were divided into three portions, and on each portion grew three gemmae derived from the same independent transformant of that promoter construct. (D) Relative thallus size (the ratio of sizes of subcellular targeting line plants: average size of WT plants) of different promoter line plants (2-week-old). In B and D, each bar represents an independent transformant for that promoter construct, and error bars represent standard deviation between three biological replicates. Letters above the bars indicate statistically significant differences between the different subcellular targeting $\text{proMpEF1}\alpha\text{:mTurquoise2}$ lines (Dunn's test; $P < 0.05$).

4 h per day for 5 d and then harvested for betanin extraction and quantification. Plants with 4-h induction produced significantly higher amount of betanin (Fig. 7) and yielded $\sim 250 \mu\text{g}$ betanin/g FW, similar to pro_{35S} lines although lower than that obtained from $\text{pro}_{35S} \times 2$ lines.

Discussion

The model liverwort *M. polymorpha* is a simple haploid plant with fast growth, short generation times and prolific capacity for reproduction. This combination with facile molecular genetic tools and easy access for high-resolution optical imaging make *Marchantia* an ideal test bed for reprogramming plant genetic systems. Promoters are essential for modulating plant gene expression, and different levels of expression are required

for construction of different genetic circuits, and for reprogramming metabolism. To date, only few promoters are well characterized for their expression pattern in *Marchantia*, and their properties have not been well compared.

We have screened a new set of high-level, widely expressed promoters and localization tags for safe accumulation of proteins and metabolites. In this study, we expanded the promoter repertoire by characterizing five new constitutive transcription factor promoters with various levels of expression across many cell types. These provide new resources for research in *Marchantia*, similar to other model systems, where a spectrum of promoters with different expression levels have been made available, such as *Escherichia coli* (Anderson collection of promoters at the Registry of Standard Biological Parts), *A. thaliana* (Jores et al. 2021) and *N. benthamiana* (Tian et al. 2022).

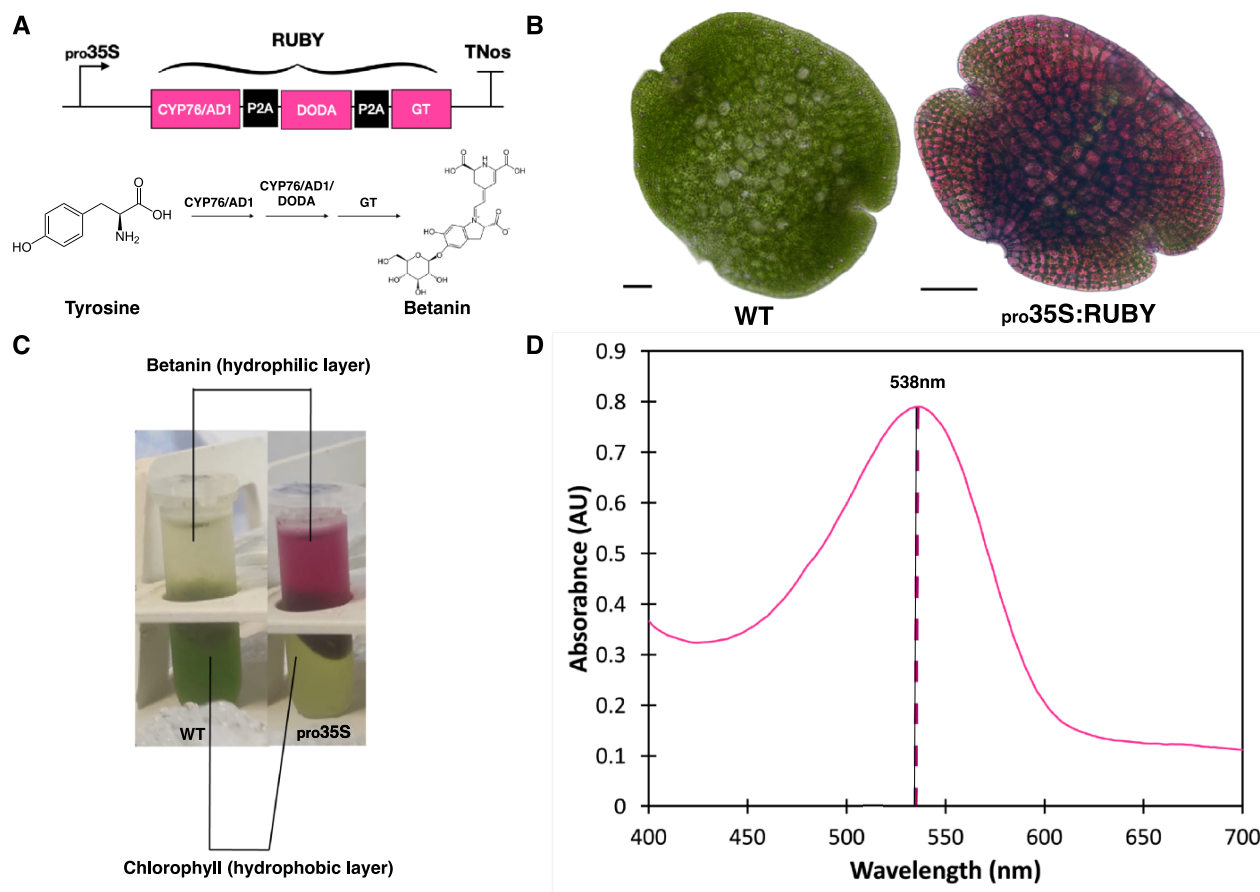


Fig. 5 Confirmation of production of betanin by expression of the *RUBY* cassette using *pro35S*. (A) Schematic representation of the *pro35S:RUBY* construct and the simplified betanin biosynthetic pathway. (B) Bright-field microscopy images of a WT gemma and a *pro35S:RUBY* gemma. Scale bar = 50 μm . (C) Extraction of chlorophyll pigments (hydrophobic layer) and betanin pigments (hydrophilic layer) from 3-week-old WT and *pro35S:RUBY* plants. (D) Absorbance spectra of the extracted betalain pigments from *pro35S:RUBY* plants. The absorbance at 538-nm for betanin (the most prominent betalain pigment) is indicated with a dashed line.

Protein targeting to various subcellular locations was previously explored in *Marchantia* (Sauret-Güeto et al. 2020, Westermann et al. 2020). However, little is known of each compartment's ability to accumulate the maximum amount of recombinant protein. We compared the yield of mTurquoise2 in various subcellular targeting lines and showed that it accumulated to the highest level when retained in the cytosol. This is at odds with some reports of recombinant protein work in flowering plants, where compartmentalization to different organelles can lead to higher recombinant protein yield (Habibi et al. 2017). This may reflect differing properties of the target protein or plant system. General principles observed in flowering plant models often do not necessarily apply to bryophytes (Niederau et al. 2024).

We used *Marchantia* promoters to drive expression of the recently published *RUBY* cassette as an example of producing enzymes for metabolic engineering. The beetroot betanin synthesis genes (He et al. 2020) were expressed without codon optimization, commonly required for efficient translation of heterologous proteins (Webster et al. 2017). This demonstrates

the feasibility of expressing foreign metabolic pathway genes in *Marchantia*. 2A peptides, which allow polycistronic expression by ribosome-skipping in plants (Khosla et al. 2020) and other systems (Liu et al. 2017), have been shown to work in *Marchantia* for expression of two fluorescent proteins in a polycistronic vector (Waller et al. 2023). We have confirmed that the same mechanism can be applied to metabolic pathway enzymes, such as those in the betanin synthesis pathway.

High levels of transgene expression are known to have physiological consequences for hosts, and termed as 'metabolic burden' (Wu et al. 2016). The allocation of resources for normal host metabolism can be altered due to the expression of transgene and accumulation of recombinant proteins/metabolic products, leading to adverse effects on growth. The phenomenon was observed in tobacco chloroplast transformants that expressed high levels of recombinant proteins (Lössl et al. 2005, Hennig et al. 2007), and in *Marchantia* where up to 50% reduction in biomass was observed in chloroplast-engineered plants expressing mTurquoise2 up to $\sim 400\text{--}500 \mu\text{g/g}$ FW (Frangedakis et al. 2021). We have made similar observations for

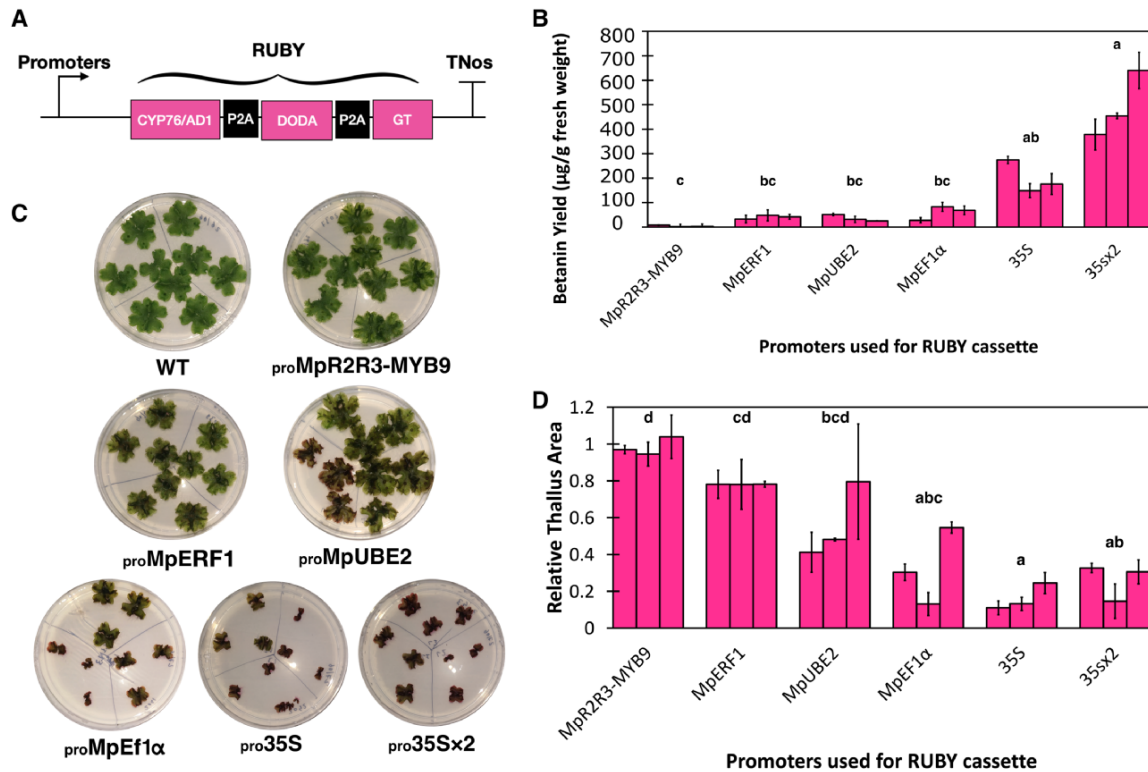


Fig. 6 Level of betanin accumulation in different promoter:RUBY lines and relative size estimation of plants from different promoter:RUBY lines. (A) Schematic representation of different promoter:RUBY constructs. (B) Betanin extracted in different promoter:RUBY lines in 3-week-old plants, in $\mu\text{g/g}$ FW. (C) Images of 2-week-old WT and different promoter:RUBY plants grown in 9-cm Petri dishes in 0.5 \times Gamborg B-5 basal medium supplemented with 0.5% (w/v) sucrose. The plates were divided into three portions, and on each portion grew three gemmae derived from the same independent transformant of that promoter construct. (D) Relative thallus size (the ratio of sizes of subcellular-targeting line plants: average size of WT plants) of different promoter:RUBY plants (2-week-old). In B and D, each bar represents an independent transformant for that promoter construct, and error bars represent standard deviation between three biological replicates. Letters above the bars indicate statistically significant differences between different promoter:RUBY lines (Dunn's test; $P < 0.05$).

plants expressing mVenus-N7 and RUBY driven by $\text{pro}_{35S \times 2}$, where plants accumulate significantly lower biomass compared to wild type (WT) plants. However, the same is not true for the cytoplasmic $\text{pro}_{35S \times 2}:\text{mTurquoise2}$ lines, where the transformants have similar growth rates to WT plants. This suggests that while high level of expression tends to lead to heavier metabolic burden, the exact effect is product-dependent and should be judged on a case-by-case basis. In addition, while $\text{pro}_{\text{MpEF1}\alpha}:\text{mTurquoise2-Lti6b}$ plants also accumulated high levels of mTurquoise2 similar to $\text{pro}_{\text{MpEF1}\alpha}:\text{mTurquoise2}$ plants, their growth was severely hindered, resulting in significantly smaller plants compared to other lines. This suggests that subcellular localization of recombinant proteins can affect the extent of burden seen in transgenic plants.

Despite significant suppression of growth, the maximum yield obtained in 3-week $\text{pro}_{35S \times 2}:\text{RUBY}$ plants was 1.5 times higher than that reported in the native producer beetroot ($\sim 300\text{--}400 \mu\text{g/g}$ FW). Slow growth due to high transgene expression was overcome by using an inducible heat-shock promoter $\text{pro}_{\text{MpHSP17.8A1}}$. The plants produced similar yields of betanin as the 3-week-old pro_{35S} lines, which have one of the

highest accumulations of betanin among the lines. This served as a proof-of-principle for the potential of inducible promoters to drive expression of recombinant protein for metabolic engineering in Marchantia. Furthermore, Marchantia provides a facile platform for cell and tissue selective expression and programming of synthetic source-sink relationships for safer high-level production of metabolites.

As a point of reference, the $\sim 60 \mu\text{g/g}$ FW of mTurquoise2 protein obtained from nuclear transformation compares with $400\text{--}500 \mu\text{g/g}$ FW of mTurquoise2 obtained from chloroplast genome transformation (Fragedakis et al. 2021). In addition, variation in yields was observed between nuclear transformed lines (Figs. 2B, 4B, 6B). This could be due to post-transcriptional RNA silencing (Matsuo and Atsumi 2019) or random insertion of the transgene cassette into the plant genome by *A. tumefaciens* (Dong and Ronald 2021). In contrast, chloroplast transformation occurs by homologous recombination into a defined chromosomal site, and gene silencing is effectively non-existent in chloroplasts. Chloroplast transformation may be the method of choice for expression of heterologous proteins, but more time consuming and less efficient than nuclear transformation

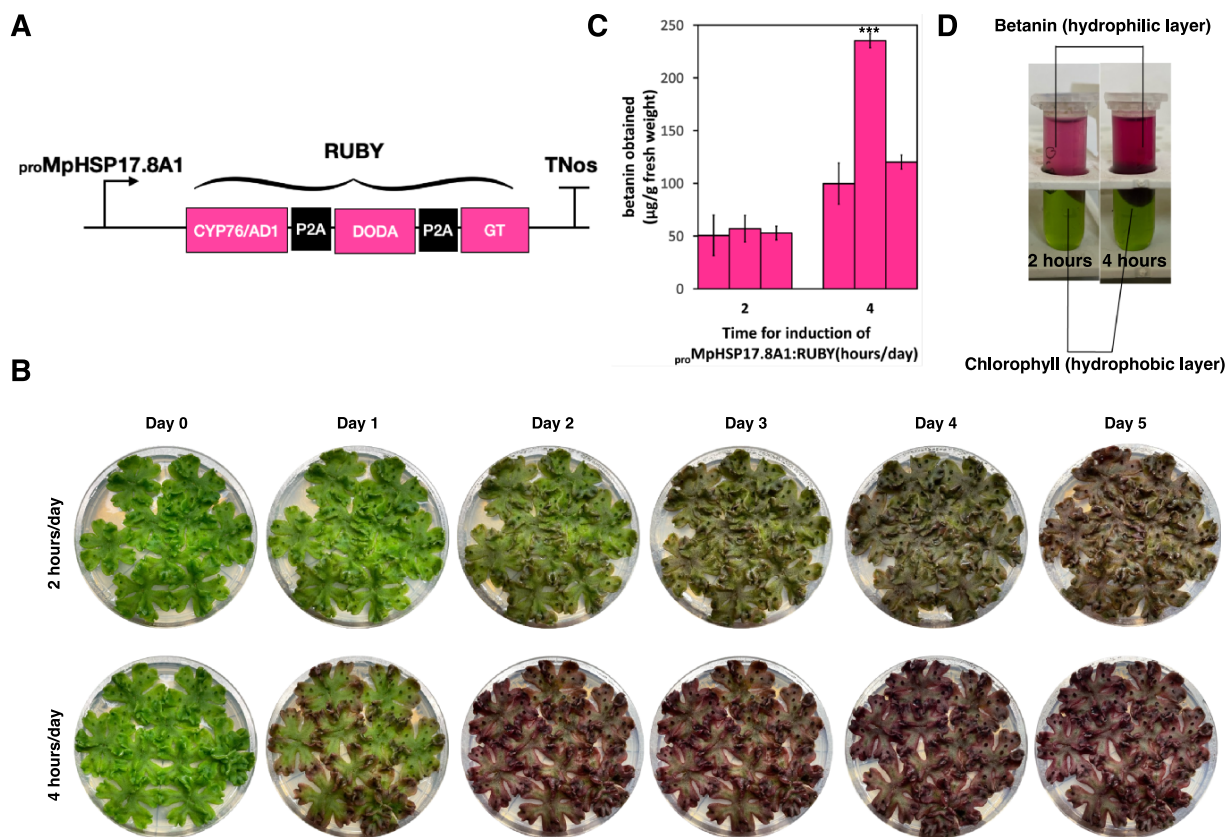


Fig. 7 Heat-shock induction of betanin accumulation in $proMpHSP17.8A1:RUBY$ lines. (A) Schematic representation of the $proMpHSP17.8A1:RUBY$ construct. P2A: ribosome skipping domain. (B) The change in thallus color in 3-week-old plants from $proMpHSP17.8A1:RUBY$ lines with 2 or 4 h of induction at 37°C across 5 d. The plants were grown in 9-cm Petri dishes in 0.5× Gamborg B-5 basal medium supplemented with 0.5% (w/v) sucrose. The plates were divided into three portions, and three gemmae derived from the same independent transformant of that promoter construct were grown on each segment. (C) Betanin yields from $proMpHSP17.8A1:RUBY$ lines with different induction times in 3-week-old plants post-induction, in $\mu\text{g/g}$ FW. Each bar represents an independent transformant for that promoter construct, and error bars represent standard deviation between three biological replicates. The triple asterisks above the bars indicate statistically significant differences between plant groups with different induction times (Wilcoxon signed-rank test, $P < 0.01$). (D) Extraction of chlorophyll pigments (hydrophobic layer) and betanin pigments (hydrophilic layer) from 3-week-old $proMpHSP17.8A1:RUBY$ lines with 2 and 4 h of induction at 37°C.

(Sauret-Güeto et al. 2020), and not even feasible for many plant species. Nuclear transformation offers more potential for inducible and tissue-specific gene expression, and it may be possible to copy natural systems, and explore specialized cell types such as trichomes and oil body cells for safe storage of metabolites at very high levels.

Apart from inducible promoters, such as the heat-shock promoter $proMpHSP17.8A1$ used in this study, more sophisticated genetic circuits can also be used to overcome metabolic burdens and improve heterologous expression. Genetic circuits driving gene expression under the control of multiple input signals and tissue-type-specific promoters have been implemented in plants (Brophy et al. 2022, Vazquez-Vilar et al. 2023). The combination of synthetic transcription factors, activator and repressor domains, tunable promoters (Cai et al. 2020) can achieve a better dynamic range of expression, with a completely silent OFF state and a hyperactive ON state. In *Marchantia*, the synthetic transcription factor GAL4-VP16 has been used (Nishihama et al. 2016), and it can potentially be used to construct orthogonal genetic circuits for enhancing recombinant protein

production. Tissue-specific promoters have a great potential for agriculture and bioproduction, targeting specific tissues or cells that could be able to direct production to harvestable organs or specialized cells (Tansley et al. 2024). Similar to trichomes in vascular plants, oil body cells have potential for cell-type-specific metabolic engineering of cytotoxic terpenoids with some already well-characterized promoters (Romani et al. 2022).

Overall, we present the *Marchantia* research community with new promoter parts to assist gene expression research with reference data, comparing their relative strength and potential for recombinant protein production and metabolic engineering.

Materials and Methods

Plant material and growth conditions

Marchantia polymorpha subs. *rudelaris* accessions Cam-1 (male) and Cam-2 (female) were used (Delmans et al. 2017). Under normal conditions, plants were grown on solid 0.5× Gamborg B-5 basal medium (Phytotech #G398) at pH

5.7–5.8 with 1.2% (w/v) agar micropropagation grade (#A296 PhytoTech Labs, Lenexa, Kansas, USA) under continuous light at 21°C with a light intensity of 150 $\mu\text{mol}/\text{m}^2/\text{s}$. The media were supplemented with 0.5% (w/v) sucrose where specified. For spore production, plants were grown in Microbox micropropagation containers (SacO_2) in long day conditions (16 h light/8 h dark) under light supplemented with far-red light as previously described (Sauret-Güeto et al. 2020).

Plasmid assembly

L0 DNA parts and mVenus constructs were obtained from the OpenPlant tool kit, described in (Sauret-Güeto et al. 2020) and (Romani et al. 2024), except L0-mTurquoise2 which was built by polymerase chain reaction using Phusion polymerase with the OpenPlant tool kit mTurquoise2-CDS12 part as template, with primers non-optimized mTurq2 F and non-optimized mTurq2 R. 35S:RUBY was a gift from Yunde Zhao (Addgene plasmid #160,908; RRID:Addgene_160908; <http://n2t.net/addgene:160908>) (He et al. 2020), and was used as a template for creating the L0-RUBY-CDS part using a protocol described previously (Sauret-Güeto et al. 2020). The L0-RUBY-CDS part was confirmed by Sanger sequencing using primers pUAP-F, pUAP-R, as well as RUBY-1,2,3. For the assembly of L3 plasmids, a new L3 acceptor (pBy_10) was built and the plasmid map is provided in the supplementary data as a GenBank file. mTurquoise2 and RUBY constructs were made by one-step Type-IIS cloning of L0 parts into the L3 acceptor pBy_10 using BsaI and T4 ligase.

For the mVenus promoter constructs, the presence of the correct insert was confirmed by restriction *XhoI* digestion (#FD0694 Thermo Fisher Scientific, UK) and by Sanger sequencing using primer Rv5. For mTurquoise2 constructs, the presence of the correct insert was confirmed by *NdeI* digestion (Thermo Scientific #FD0583), and by Sanger sequencing using primers Ef1a-seq-2 and Nos-35S-seq-2. L3-RUBY constructs were confirmed by *XhoI* digestion and Sanger sequencing using the primer RUBY-seq-4.

Agrobacterium-mediated transformation

Marchantia spores were sterilized as previously described (Sauret-Güeto et al. 2020). A modification of the published *Agrobacterium*-mediated protocol for transformation in six-well plates (Sauret-Güeto et al. 2020) was used, as described previously (Romani et al. 2024).

Laser scanning confocal microscopy

For mVenus lines, images were acquired on a Leica SP5 confocal microscope upright system equipped with an Argon ion gas laser with emitted wavelengths of 458, 476, 488 and 514 nm and a

405 nm diode laser, a 594 nm HeNe laser, a 633 nm HeNe laser and a 561 DPSS laser. Imaging was conducted either using a 10 \times air objective (HC PL APO 675 10 \times /0.40 CS2) or a 2.5 \times air objective (HC PL APO 20 \times /0.75 CS2). Sequential scanning mode was selected for observing fluorescent proteins with overlapping emission spectra. Excitation laser wavelengths and emission fluorescence bandwidth windows were as follows: for mVenus (514 nm, 527–552 nm), for mScarlet (561 nm, 595–620 nm) and for chlorophyll autofluorescence (633 nm, 687–739 nm).

For mTurquoise2 lines, images were acquired on an upright Leica SP8X confocal microscope equipped with a 460–670 nm supercontinuum white light laser, two continuous wave laser lines of 405 nm and 442 nm and a five-channel spectral scanhead (four hybrid detectors and one photomultiplier). Imaging was conducted using either a 20 \times air objective (HC PL APO 20 \times /0.75 CS2) or a 40 \times water immersion objective (HC PL APO 40 \times /1.10 W CORR CS2). Excitation laser wavelength and fluorescence emission bandwidth windows were as follows: 442 nm and 460–485 nm (for mTurquoise2) and 488 or 515 nm and 670–700 nm (for chlorophyll autofluorescence). Chlorophyll autofluorescence was imaged simultaneously with mTurquoise2.

Protein extraction and yield estimation

mVenus and mTurquoise2 standard curves (random fluorescence unit against known protein concentration) were built as previously described using bacterial-expressed mVenus-7xHis-tagged and mTurquoise2-6xHis-tagged proteins (Frangedakis et al. 2021) for the estimation of the quantity of each fluorescent protein expressed in plant samples.

Marchantia thallus tissue (200 mg) from 3-week-old plants was ground on ice with a mortar and pestle and resuspended in 700 μl of protein extraction buffer [50 mM Tris-HCl, pH 7.5, 150 mM NaCl, Tween 20 0.1% (v/v), 10% (v/v) glycerol, 1 mM dithiothreitol (DTT)] plus Roche cOmplete protease inhibitor (#11836170001, Roche Diagnostics, Mannheim, Germany). Plant debris was pelleted by centrifugation (15 min, 15,000 r.p.m., 4°C), and the supernatant was treated as the total soluble protein fraction. Three replicates of 20 μl of extract for each sample were used for measuring fluorescence in a Sterilin™ Clear Microtiter™ Plate (#611V96, Thermo Fisher Scientific, UK). A BMG CLARIOstar plate reader was used with an excitation and emission wavelength appropriate for mTurquoise2 measurement (excitation: 430–20 nm, emission: 474–20 nm, gain 500 nm). Sample values were adjusted by subtracting the fluorescence values of the blank.

Estimation of plant sizes

To estimate plant sizes and growth, the projection area was calculated using overhead pictures of Petri dishes containing 12 (three biological replicates per independent transgenic line) 2-week-old *Marchantia* plants. Pictures were scaled and the projected area of each individual plant was manually selected and measured using the Measure tool in ImageJ/Fiji (Schneider et al. 2012). For plots, data were normalized to the ratio of the thallus area of transgenic plants to WT plants.

Betanin extraction and quantification

The betanin extraction method was adapted from a previously published protocol (Chang et al. 2021). Briefly, 200 mg of 3-week-old plant tissue was placed into a 2-ml Eppendorf tube with a stainless-steel bead (3–7 mm diameter), flash-frozen in liquid nitrogen, and subjected to disruption for two cycles of 1 min at 30 Hz on a TissueLyser II (Qiagen, Manchester, UK) at 4°C. Betanin pigments were then extracted with 2 ml of extraction solution [methanol:chloroform:water (1:2:1), supplemented with 1 mM of ascorbic acid], followed by 10 s of vigorous vortexing, followed by centrifugation (2 min, 4°C, 13,000 r.p.m.). After centrifugation, triplicates of 100 μl each from the upper (hydrophilic) layer were collected and dispensed into a black-walled 96-well tissue culture treated plate with a lid (#655090 Greiner Bio-One, Stonehouse, UK). A BMG CLARIOstar plate reader was used for measurement of absorbance across the full spectrum (220–975 nm) and at three particular wavelengths [538 nm for betanin absorbance, 900 nm and 975 nm for correction of path length (Lampinen et al. 2012)].

Induction of heat-inducible promoter lines

Three gemmae from each of the three independent transformants with the heat-inducible promoter-driven RUBY cassette were grown on Gamborg B-5 plates for 3 weeks. The plants were placed in a 37°C incubator without light for 2 or 4 h each day at the same time, respectively, before being moved back to the standard growth conditions. After 5 d, plants were harvested and flash-frozen in liquid nitrogen, before being subjected to the betanin extraction protocol above.

Data handling

Data were expressed as the means \pm standard deviation. Statistical analysis was performed using R Statistical Software (R Core Team 2023). Differences between two groups were assessed using a Wilcoxon signed-rank test. For multiple comparisons, significance analysis was determined by Kruskal–Wallis

one-way analysis of variance, followed by a post hoc Dunn's test (Bonferroni correction for the final *P*-value) using the R FSA package (Ogle et al. 2023). Letter summaries of statistical similarities and differences were compiled using the R multcompView (Graves et al. 2023) and rcompanion packages (Mangiafico 2023).

Supplementary Data

Supplementary data are available at PCP online.

Data Availability

Promoter sequences are available at <https://mpexatdb.org> (Romani et al. 2024). All primer sequences are provided in the supplementary data.

Funding

This work was funded as part of the BBSRC/EPSRC Open-Plant Synthetic Biology Research Centre (grant BB/L014130/1 to J.H.), BBSRC BB/F011458/1 for confocal microscopy, (BBSRC BB/T007117/1 to J.H.) and the Doris Zimmern HKU-Cambridge Hughes Hall Scholarship (to S.W.T.).

Acknowledgments

We thank William Boxall for his advice on the statistical analysis and R programming.

Disclosures

The authors have no conflicts of interest to declare.

References

- Althoff, F., Kopischke, S., Zobell, O., Ide, K., Ishizaki, K., Kohchi, T., et al. (2014) Comparison of the MpEF1 α and CaMV35 promoters for application in *Marchantia polymorpha* overexpression studies. *Transgenic Res.* 23: 235–244.
- Amack, S.C. and Antunes, M.S. (2020) CaMV35S promoter – a plant biology and biotechnology workhorse in the era of synthetic biology. *Curr. Plant Biol.* 24: 100179.
- Bankar, S.B., Bule, M.V., Singhal, R.S. and Ananthanarayan, L. (2009) Glucose oxidase—an overview. *Biotechnol. Adv.* 27: 489–501.
- Bowman, J.L., Arteaga-Vazquez, M., Berger, F., Briginshaw, L.N., Carella, P., Aguilar-Cruz, A., et al. (2022) The renaissance and enlightenment of *Marchantia* as a model system. *Plant Cell* 34: 3512–3542.
- Brophy, J.A.N., Magallon, K.J., Duan, L., Zhong, V., Ramachandran, P., Kniazev, K., et al. (2022) Synthetic genetic circuits as a means of reprogramming plant roots. *Science* 377: 747–751.
- Brückner, K., Schäfer, P., Weber, E., Grützner, R., Marillonnet, S., and Tissier, A. (2015) A library of synthetic transcription activator-like effector-activated promoters for coordinated orthogonal gene expression in plants. *Plant J.* 82: 707–716.
- Cai, Y.-M., Kallam, K., Tidd, H., Gendarini, G., Salzman, A. and Patron, N. (2020) Rational design of minimal synthetic promoters for plants. *Nucleic Acids Res.* 48: 11845–11856.
- Chang, Y.-C., Chiu, Y.-C., Tsao, N.-W., Chou, Y.-L., Tan, C.-M., Chiang, Y.-H., et al. (2021) Elucidation of the core betalain biosynthesis pathway in *Amaranthus tricolor*. *Sci. Rep.* 11: 6086.
- Chen, N., Yu, Z.-H. and Xiao, X.-G. (2017) Cytosolic and nuclear co-localization of betalain biosynthetic enzymes in tobacco suggests that betalains are synthesized in the cytoplasm and/or nucleus of betalainic plant cells. *Front. Plant Sci.* 8: 242166.
- de Felipe, P., Luke, G.A., Brown, J.D. and Ryan, M.D. (2010) Inhibition of 2A-mediated 'cleavage' of certain artificial polyproteins bearing N-terminal signal sequences. *Biotechnol. J.* 5: 213–223.
- Delmans, M., Pollak, B. and Haseloff, J. (2017) MarpoDB: an open registry for *Marchantia polymorpha* genetic parts. *Plant Cell Physiol.* 58: e5.
- DeLoache, W.C., Russ, Z.N., Narcross, L., Gonzales, A.M., Martin, V.J.J. and Dueber, J.E. (2015) An enzyme-coupled biosensor enables (S)-reticuline production in yeast from glucose. *Nat. Chem. Biol.* 11: 465–471.
- Dong, O.X. and Ronald, P.C. (2021) Targeted DNA insertion in plants. *Proc. Natl. Acad. Sci. USA* 118: e2004834117.
- Dugdale, B., Mortimer, C.L., Kato, M., James, T.A., Harding, R.M. and Dale, J.L. (2013) In plant activation: an inducible, hyperexpression platform for recombinant protein production in plants. *Plant Cell.* 25: 2429–2443.
- Engler, C., Youles, M., Gruetzner, R., Ehnert, T.-M., Werner, S., Jones, J.D.G., et al. (2014) A golden gate modular cloning toolbox for plants. *ACS Synth. Biol.* 3: 839–843.
- Feng, Z., Li, X., Fan, B., Zhu, C., and Chen, Z. (2022) Maximizing the production of recombinant proteins in plants: from transcription to protein stability. *Int. J. Mol. Sci.* 23: 13516.
- Finka, A., Saidi, Y., Goloubinoff, P., Neuhaus, J.-M., Zrýd, J.-P. and Schaefer, D.G. (2008) The knock-out of ARP3a gene affects F-actin cytoskeleton organization altering cellular tip growth, morphology and development in moss *Physcomitrella patens*. *Cell Motil. Cytoskeleton* 65: 769–784.
- Frangedakis, E., Guzman-Chavez, F., Rebmann, M., Markel, K., Yu, Y., Per-raki, A., et al. (2021) Construction of DNA tools for hyperexpression in *Marchantia* chloroplasts. *ACS Synth. Biol.* 10: 1651–1666.
- Gils, M., Kandzia, R., Marillonnet, S., Klimyuk, V. and Gleba, Y. (2005) High-yield production of authentic human growth hormone using a plant virus-based expression system. *Plant Biotechnol. J.* 3: 613–620.
- Graves, S., Piepho, H.-P. and Selzer, L. (2023) Visualizations of paired comparisons. <https://cran.r-project.org/web/packages/multcompView/multcompView.pdf> (December 10, 2023, date last accessed).
- Grützner, R., Schubert, R., Horn, C., Yang, C., Vogt, T. and Marillonnet, S. (2021) Engineering betalain biosynthesis in tomato for high level betanin production in fruits. *Front. Plant Sci.* 12: 682443.
- Habibi, P., Prado, G.S., Pelegrini, P.B., Hefferon, K.L., Soccol, C.R. and Grossi-de-sa, M.F. (2017) Optimization of inside and outside factors to improve recombinant protein yield in plant. *Plant Cell Tissue Organ Cult.* 130: 449–467.
- Han, Y.-J., Kim, Y.-M., Hwang, O.-J. and Kim, J.-I. (2015) Characterization of a small constitutive promoter from *Arabidopsis* translationally controlled tumor protein (AtTCTP) gene for plant transformation. *Plant Cell Rep.* 34: 265–275.
- He, Y., Zhang, T., Sun, H., Zhan, H. and Zhao, Y. (2020) A reporter for non-invasively monitoring gene expression and plant transformation. *Hortic. Res.* 7: 152.
- Hennig, A., Bonfig, K., Roitsch, T. and Warzecha, H. (2007) Expression of the recombinant bacterial outer surface protein A in tobacco chloroplasts leads to thylakoid localization and loss of photosynthesis. *FEBS J.* 274: 5749–5758.
- Holtorf, S., Apel, K. and Bohlmann, H. (1995) Comparison of different constitutive and inducible promoters for the overexpression of transgenes in *Arabidopsis thaliana*. *Plant Mol. Biol.* 29: 637–646.
- Ishizaki, K., Chiyoda, S., Yamato, K.T. and Kohchi, T. (2008) *Agrobacterium*-mediated transformation of the haploid liverwort *Marchantia polymorpha* L., an emerging model for plant biology. *Plant Cell Physiol.* 49: 1084–1091.

- Ishizaki, K., Nishihama, R., Ueda, M., Inoue, K., Ishida, S., Nishimura, Y., et al. (2015) Development of gateway binary vector series with four different selection markers for the liverwort *Marchantia polymorpha*. *PLoS One* 10: e0138876.
- Jiang, P., Zhang, K., Ding, Z., He, Q., Li, W., Zhu, S., et al. (2018) Characterization of a strong and constitutive promoter from the *Arabidopsis* serine carboxypeptidase-like gene AtSCPL30 as a potential tool for crop transgenic breeding. *BMC Biotech.* 18: 59.
- Jores, T., Tonnies, J., Wrightsman, T., Buckler, E.S., Cuperus, J.T., Fields, S., et al. (2021) Synthetic promoter designs enabled by a comprehensive analysis of plant core promoters. *Nat. Plants* 7: 842–855.
- Khosla, A., Rodriguez-Furlan, C., Kapoor, S., Van Norman, J.M. and Nelson, D.C. (2020) A series of dual-reporter vectors for ratiometric analysis of protein abundance in plants. *Plant Direct.* 4: e00231.
- Lampinen, J., Raitio, M., Perälä, A. and Oranen, H. (2012) Microplate based pathlength correction method for photometric DNA quantification assay. *Vantaa: Thermo Fisher Application Note.*
- Liu, H. and Timko, M.P. (2022) Improving protein quantity and quality—the next level of plant molecular farming. *Int. J. Mol. Sci.* 23: 1326.
- Liu, Z., Chen, O., Wall, J.B.J., Zheng, M., Zhou, Y., Wang, L., et al. (2017) Systematic comparison of 2A peptides for cloning multi-genes in a polycistronic vector. *Sci. Rep.* 7: 2193.
- Lössl, A., Bohmert, K., Harloff, H., Eibl, C., Mühlbauer, S. and Koop, H.-U. (2005) Inducible trans-activation of plastid transgenes: expression of the R. eutrophaphb operon in transplastomic tobacco. *Plant Cell Physiol.* 46: 1462–1471.
- Mangiafico, S.S. (2023) Rcompanion: functions to support extension education program evaluation. Rutgers Cooperative Extension, New Brunswick, New Jersey. <https://CRAN.R-project.org/package=rcompanion/> (December 12, 2023, date last accessed).
- Marillonnet, S., Giritch, A., Gils, M., Kandzia, R., Klimyuk, V. and Gleba, Y. (2004) In planta engineering of viral RNA replicons: efficient assembly by recombination of DNA modules delivered by *Agrobacterium*. *Proc. Natl. Acad. Sci. USA* 101: 6852–6857.
- Matsuo, K. and Atsumi, G. (2019) CRISPR/Cas9-mediated knockout of the RDR6 gene in *Nicotiana benthamiana* for efficient transient expression of recombinant proteins. *Planta* 250: 463–473.
- Muthamilselvan, T., Kim, J.S., Cheong, G. and Hwang, I. (2019) Production of recombinant proteins through sequestration in chloroplasts: a strategy based on nuclear transformation and post-translational protein import. *Plant Cell Rep.* 38: 825–833.
- Niederau, P.A., Eglé, P., Willig, S., Parsons, J., Hoernstein, S.N.W., Decker, E.L., et al. (2024) Multifactorial analysis of terminator performance on heterologous gene expression in *Physcomitrella*. *Plant Cell Rep.* 43: 43.
- Nishihama, R., Ishida, S., Urawa, H., Kamei, Y., Kohchi, T., et al. (2016) Conditional gene expression/deletion systems for *Marchantia polymorpha* using its own heat-shock promoter and Cre/loxP-mediated site-specific recombination. *Plant Cell Physiol.* 57: 271–280.
- Ogle, D.H., Doll, J.C., Powell Wheeler, A. and Dinno, A. (2023) FSA: simple fisheries stock assessment methods. <https://CRAN.R-project.org/package=FSA> (December 10, 2023, date last accessed).
- Patron, N.J., Orzaez, D., Marillonnet, S., Warzecha, H., Matthewman, C., Youles, M., et al. (2015) Standards for plant synthetic biology: a common syntax for exchange of DNA parts. *New Phytol.* 208: 13–19.
- R Core Team (2023) R: A language and environment for statistical computing. R foundation for statistical computing, Vienna, Austria. <https://www.R-project.org> (December 10, 2023, date last accessed).
- Romani, F., Flores, J.R., Tolopka, J.I., Suárez, G., He, X. and Moreno, J.E. (2022) Liverwort oil bodies: diversity, biochemistry, and molecular cell biology of the earliest secretory structure of land plants. *J. Exp. Bot.* 73: 4427–4439.
- Romani, F., Sauret-Güeto, S., Rebmann, M., Annese, D., Bonter, I., Tomaselli, M., et al. (2024) The landscape of transcription factor promoter activity during vegetative development in *Marchantia*. *Plant Cell.* 36: 2140–2159.
- Saberianfar, R., Joensuu, J.J., Conley, A.J. and Menassa, R. (2015) Protein body formation in leaves of *Nicotiana benthamiana*: a concentration-dependent mechanism influenced by the presence of fusion tags. *Plant Biotechnol. J.* 13: 927–937.
- Saidi, Y., Schaefer, D.G., Goloubinoff, P., Zrýd, J.-P. and Finka, A. (2009) The CaMV 35S promoter has a weak expression activity in dark grown tissues of moss *Physcomitrella patens*. *Plant Signal. Behav.* 4: 457–459.
- Sauret-Güeto, S., Frangedakis, E., Silvestri, L., Rebmann, M., Tomaselli, M., Markel, K., et al. (2020) Systematic tools for reprogramming plant gene expression in a simple model, *Marchantia polymorpha*. *ACS Synth. Biol.* 9: 864–882.
- Schneider, C.A., Rasband, W.S. and Eliceiri, K.W. (2012) NIH image to imageJ: 25 years of image analysis. *Nat. Methods* 9: 671–675.
- Takemura, M., Kanamoto, H., Nagaya, S. and Ohyama, K. (2013) Bioproduction of prostaglandins in a transgenic liverwort, *Marchantia polymorpha*. *Transgenic Res.* 22: 905–911.
- Tansley, C., Patron, N.J. and Guiziou, S. (2024) Engineering plant cell fates and functions for agriculture and industry. *ACS Synth. Biol.* 13: 998–1005.
- Teh, Y.-H.A. and Kavanagh, T.A. (2010) High-level expression of Camelid nanobodies in *Nicotiana benthamiana*. *Transgenic Res.* 19: 575–586.
- Tian, C., Zhang, Y., Li, J. and Wang, Y. (2022) Benchmarking intrinsic promoters and terminators for plant synthetic biology research. *Biodes. Res.* 2022: 9834989.
- Vazquez-Vilar, M., Selma, S., Orzaez, D. and Yang, J.-S. (2023) The design of synthetic gene circuits in plants: new components, old challenges. *J. Exp. Bot.* 74: 3791–3805.
- Villao-Uzho, L., Chávez-Navarrete, T., Pacheco-Coello, R., Sánchez-Timm, E. and Santos-Ordóñez, E. (2023) Plant promoters: their identification, characterization, and role in gene regulation. *Genes* 14: 1226.
- Waller, M., Frangedakis, E., Marron, A.O., Sauret-Güeto, S., Rever, J., Sabbagh, C.R.R., et al. (2023) An optimized transformation protocol for *Anthoceros agrestis* and three more hornwort species. *Plant J.* 114: 699–718.
- Webster, G.R., Teh, A.Y.-H. and Ma, J.K.-C. (2017) Synthetic gene design—the rationale for codon optimization and implications for molecular pharming in plants. *Biotechnol. Bioeng.* 114: 492–502.
- Westermann, J., Koebeke, E., Lentz, R., Hülskamp, M. and Boisson-Dernier, A. (2020) A comprehensive toolkit for quick and easy visualization of marker proteins, protein–protein interactions and cell morphology in *Marchantia polymorpha*. *Front. Plant Sci.* 11: 569194.
- Wu, G., Yan, Q., Jones, J.A., Tang, Y.J., Fong, S.S. and Koffas, M.A.G. (2016) Metabolic burden: cornerstones in synthetic biology and metabolic engineering applications. *Trends Biotechnol.* 34: 652–664.
- Yang, E.J.Y. and Nemhauser, J.L. (2023) Building a pipeline to identify and engineer constitutive and repressible promoters. *Quant. Plant. Biol.* 4: e12.
- Zhao, Y. (2023) The RUBY reporter – Zhao lab. <https://zhaolab.biosci.ucsd.edu/ruby/> (December 10, 2023, date last accessed).